Mechanism for alternating access in neurotransmitter transporters

Lucy R. Forrest*[†‡], Yuan-Wei Zhang[†§], Miriam T. Jacobs[§], Joan Gesmonde[§], Li Xie*, Barry H. Honig*[¶], and Gary Rudnick[§¶]

*Howard Hughes Medical Institute, Center for Computational Biology and Bioinformatics and Department of Biochemistry and Molecular Biophysics, Columbia University, 1130 St. Nicholas Avenue, Room 815, New York, NY 10032; and [§]Department of Pharmacology, Yale University School of Medicine, 333 Cedar Street, New Haven, CT 06520-8066

Contributed by Barry H. Honig, May 16, 2008 (sent for review April 21, 2008)

Crystal structures of LeuT, a bacterial homologue of mammalian neurotransmitter transporters, show a molecule of bound substrate that is essentially exposed to the extracellular space but occluded from the cytoplasm. Thus, there must exist an alternate conformation for LeuT in which the substrate is accessible to the cytoplasm and a corresponding mechanism that switches accessibility from one side of the membrane to the other. Here, we identify the cytoplasmic accessibility pathway of the alternate conformation in a mammalian serotonin transporter (SERT) (a member of the same transporter family as LeuT). We also propose a model for the cytoplasmic-facing state that exploits the internal pseudosymmetry observed in the crystal structure. LeuT contains two structurally similar repeats (TMs1–5 and TMs 6–10) that are inverted with respect to the plane of the membrane. The conformational differences between them result in the formation of the extracellular pathway. Our model for the cytoplasm-facing state exchanges the conformations of the two repeats and thus exposes the substrate and ion-binding sites to the cytoplasm. The conformational change that connects the two states primarily involves the tilting of a 4-helix bundle composed of transmembrane helices 1, 2, 6, and 7. Switching the tilt angle of this bundle is essentially equivalent to switching the conformation of the two repeats. Extensive mutagenesis of SERT and accessibility measurements, using cysteine reagents, are accommodated by our model. These observations may be of relevance to other transporter families, many of which contain internal inverted repeats.

alternating access mechanism | neurotransmitter:sodium symporters | serotonin | structural modeling | structural repeats

Transporter-mediated movement of solutes across membranes is understood to involve an alternating access mechanism in which conformational changes alternately expose a central binding site for one or more substrates to each side of the membrane (1). Despite wide acceptance of the general features of this model, specific mechanisms that produce conformations with differing accessibility in transport proteins are largely unknown. Unlike ATP-coupled transporters such as the SERCA Ca^{2+} pump, where multiple crystal structures provide insight into many of the conformational states that constitute the reaction cycle (2, 3), the handful of structures from carrier-type transporters (uniporters, symporters, and antiporters) provide only a single conformation of each protein, with the substrate binding site exposed only to one side of the membrane (4–11). In the case of lactose permease, extensive labeling and biophysical measurements in the presence and absence of substrate have led to a proposed mechanism of conformational change exposing the substrate site to either side of the membrane (12–14), but this case is an exception to the general dearth of transporter mechanisms.

In the alternating access model, a central binding site for substrates is connected to the two sides of the membrane by permeation pathways, only one of which is accessible at a time. The crystal structure of LeuT (9) provides an example of a structure where the binding site is exposed to only one side of the membrane, in this case to the extracellular surface. LeuT has provided a useful structural model for members of the neurotransmitter sodium symporter (NSS) family (9, 15). These proteins include transporters mediating the reuptake of neurotransmitters and amino acids. Transporters for the amine neurotransmitters dopamine, norepinephrine, and serotonin are targets for important therapeutic agents and drugs of abuse, including antidepressants, cocaine, and amphetamines. The structural basis for the function of these proteins and their interactions with drugs has been a topic of intense recent interest (16, 17).

The LeuT structure contains a topologically inverted repeat of two structural elements (TMs 1–5 and TMs 6–10) that are pseudosymmetrical with respect to the plane of the membrane (Fig. 1). This feature suggests the possibility that corresponding structural elements from the two repeats might form the two alternative permeation pathways that lead to one side of the membrane or the other. Analysis of the LeuT structure reveals that members of both repeats, TMs 1b and 3 in the first and TMs 6a and 10 in the second repeat, contribute to an aqueous vestibule that is exposed to the extracellular surface of the protein (Fig. 1) (9). Each of these helices has a corresponding topologically inverted helix in the other structural repeat, that is, TMs 6b, 8, 1a, and 5, respectively. The residues in these helices are buried in the crystal structure, but the symmetry arguments raised here suggest that they are exposed in the alternate, cytoplasm-facing conformation of the transporter.

Consistent with the structure of LeuT, in the homologous serotonin transporter (SERT), TM10 was shown to be accessible to extracellular reagents (18). Conversely, in SERT, methanethiosulfonate (MTS) reagents applied from the cytoplasmic side of the membrane reacted rapidly with cysteine residues introduced into the cytoplasmic half of TM5, which corresponds to TM10 in the second repeat (19). These reactive positions were proposed to contribute to the cytoplasmic substrate permeation pathway because their reactivity was modulated by substrates (serotonin, Na^+ and Cl^-) and an inhibitor (cocaine) in a manner consistent with the effects of these ligands in the transport cycle (20). Moreover, ibogaine, an hallucinogenic alkaloid proposed to bind preferentially to the cytoplasm-facing state of SERT, induced a concerted conformational change leading to increased accessibility of the reactive

Author contributions: L.R.F. and G.R. designed research; L.R.F., Y.-W.Z., M.T.J., J.G., and L.X. performed research; L.R.F. analyzed data; and L.R.F., B.H.H., and G.R. wrote the paper.

The authors declare no conflict of interest.

Freely available online through the PNAS open access option.

[†]L.R.F. and Y.W.Z. contributed equally to this work

[‡]Present address: Computational Structural Biology Group, Max Planck Institute of Biophysics, Max-von-Laue-Str. 3, 60438 Frankfurt am Main, Germany.

[¶]To whom correspondence may be addressed. E-mail: bh6@columbia.edu or gary.rudnick@yale.edu.

This article contains supporting information online at www.pnas.org/cgi/content/full/0804659105/DCSupplemental.

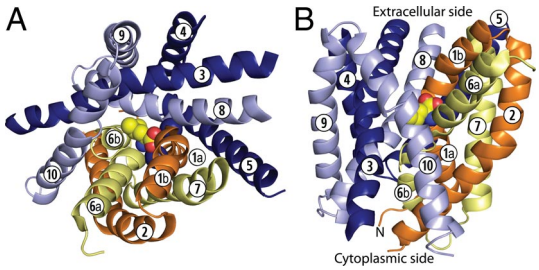

Fig. 1. Crystal structure of LeuT viewed from the extracellular side (*A*) and in the plane of the membrane (*B*). The leucine substrate and sodium ions are shown in spheres. Transmembrane domains from the first repeat (1–5) are shown in darker colors (orange and dark blue), and those from the second repeat (6–10) are in lighter colors (yellow and pale blue). The two structural repeats are divided up to form a bundle (yellow and orange) cradled within a scaffold (pale and dark blue).

positions in TM5 and decreased reactivity of residues in the extracellular permeation pathway (21).

To better define the cytoplasmic pathway, we have examined the cytoplasmic accessibility of residues in helices 6b, 8 and 1a in SERT in addition to TM5 (20, 21). Our results suggest that the cytoplasmic vestibule is formed by the topologically inverted helices corresponding to those that form the extracellular vestibule, which is consistent with the internal symmetry of the protein. On this basis, we have constructed a detailed structural model of the cytoplasm-facing state of LeuT, which is essentially an inverted form of the extracellular-facing state. Comparison of the two structures reveals a simple mechanism for the conformational change that connects the two states. The central assumption of this mechanism is that alternating accessibility results from switching between alternative conformations of the two structural repeats. The consistency between the structural model and the experimental data supports this conformational switching mechanism of transport. Moreover, because sequence analysis reveals the presence of repeating elements in other transporter families (22, 23), the exchange of alternate conformations between internal repeats may well prove to be a transport mechanism of quite general relevance.

Results

Identification of Residues in the Cytoplasmic Permeation Pathway of SERT. We created 36 SERT mutants in which cysteine replaced 11 residues in TM1, 5 in TM3, 8 in TM6, and 12 residues in TM8. For each of these mutants, we first measured the sensitivity of serotonin transport in intact cells to 2-(aminoethyl)-methanethiosulfonate hydrobromide (MTSEA). Previous results with this MTSEA in this system demonstrated that intracellular cysteine residues were modified very poorly (24) despite the permeability of MTSEA in model systems (25). With two exceptions, MTSEA did not inhibit these mutants in intact cells, consistent with their location in the cytoplasmic pathway [supporting information (SI) Table S1]. Y95C (26) and A441C, which were sensitive to MTSEA, are apparently close enough to the binding site region to be accessible from the extracellular side of the membrane.

We measured the accessibility of these positions from the cytoplasmic side of the protein, using membrane preparations from cells expressing these mutants. In these membrane preparations, both cytoplasmic and extracellular faces are accessible to ligands and MTS reagents (20). Specifically, binding of the cocaine analogue 2β-2-carbomethoxy-3-(4-iodophenyl)tropane (β-CIT), was inhibited by MTS reagents that modified TM5 residues in the cytoplasmic permeation pathway (20). This inactivation is attributed to conformational restrictions, imposed by adding bulk and charge within the cytoplasmic pathway, that prevent SERT from assuming the extracellular-facing state to which cocaine and its analogues, such as β-CIT, bind. Similar inactivation of β-CIT binding by MTS reagents is observed for each of the TM1, -6, and -8 mutants. As shown in Fig. 2, individual rates of inactivation (red and blue lines in *Upper*) vary by at least 100-fold within each of these TMs (see *SI Text* and Fig. S1), even though most of these cysteines are at positions predicted by the LeuT crystal structure to be buried, some quite deep within the protein. (Green lines in Fig. 2 refer to accessibility predictions from a model discussed below.)

The ability to pharmacologically manipulate the conformation of SERT provides a powerful tool for extending these results. Accordingly, reactive mutants were further analyzed by measuring the effect of cocaine and ibogaine on their reactivity (Fig. 2, *Lower*). Cocaine is expected to stabilize the extracellular state of SERT, in which the cytoplasmic pathway is closed (20); consistent with this expectation, cocaine decreased reactivity for the majority (11 of 13) of the most reactive mutants by 2- to 28-fold (Fig. 2 and Fig. S2). Ibogaine, in contrast, is expected to stabilize the cytoplasm-facing state and to open the cytoplasmic pathway (21); accordingly, ibogaine was found to increase the reactivity of most (11 of 13) of the same mutants by 1.4- to 6.9-fold (Figs. 2, S2). Two exceptions were positions near the extreme cytoplasmic ends of TMs 5 and 8, which may never be entirely inaccessible.

The first intracellular loop (IL1) contains two positively charged residues (Arg-152 and Lys-153) in proximity to TM6 (and to a lesser extent TM8). Accordingly, cysteines placed at some TM6 positions, particularly 347, reacted faster with the negatively charged (2-sulfonatoethyl)methanethiosulfonate (MTSES) than with MTSEA (Fig. 2 and Table S2) despite the 6- to 8-fold intrinsically higher reactivity of MTSEA with monoanionic thiols, such as cysteine (27). Likewise, MTSEA and MTSES reacted at comparable rates with TM8 cysteine residues (Fig. 2 and Table S2). We attribute the anomalous reactivity of these cysteines to an electrostatic effect of the positive charges in IL1 that biases their relative reactivity toward MTSES rather than MTSEA.

Taken together with previous results, the accessibility data define a permeation pathway, formed by TM1, -5, -6, and -8, that links the substrate binding site with the cytoplasm (Fig. 3). To test for other possible permeation pathways, we measured the accessibility of five positions in the cytoplasmic half of TM3, 164 through 168, which contact TMs 10 and 12 and the unreactive faces of TMs 6 and 8 in the crystal structures (Fig. 3). Each of these cysteine replacement mutants was relatively insensitive to MTSEA, with inactivation rate constants significantly lower than 0.1 $M^{-1}\cdot sec^{-1}$. These results further reduce the possibility of a permeation pathway that does not involve TM1, -5, -6 and -8.

Modeling the Cytoplasm-Facing State of LeuT. To elucidate in atomic detail the conformational changes that open the cytoplasmic permeation pathway, we examined the internal symmetry of the LeuT structure. As shown by Yamashita *et al.* (9), TMs 1–5 can be superimposed on TMs 6–10 with an rmsd of 4.7 Å by a rotation of ≈180°. We found that splitting the repeats into two parts consisting of either the first two or the last three TMs in each repeat led to significantly improved fits with rmsd values of 3.4 and 3.2 Å, respectively (see *SI Text*). This result suggested that the difference in conformation between the two repeats is a consequence of a difference in orientation of the first two TMs relative to the rest of the TMs in the repeat. This is illustrated in Fig. 4, which shows TMs 3–5 superimposed on TMs 8–10. The orientation of TMs 1–2 (blue) is tilted by ≈30° with respect to TMs 6–7 (red) around an axis in the plane of the membrane that runs through the Cα atom of Val-23.

In the LeuT structure, the first two TMs of each structural repeat (TM1, -2, -6, and -7) form a four-helix bundle, distorted by the nonhelical regions in the middle of TM1 and -6, and

BIOCHEMISTRY

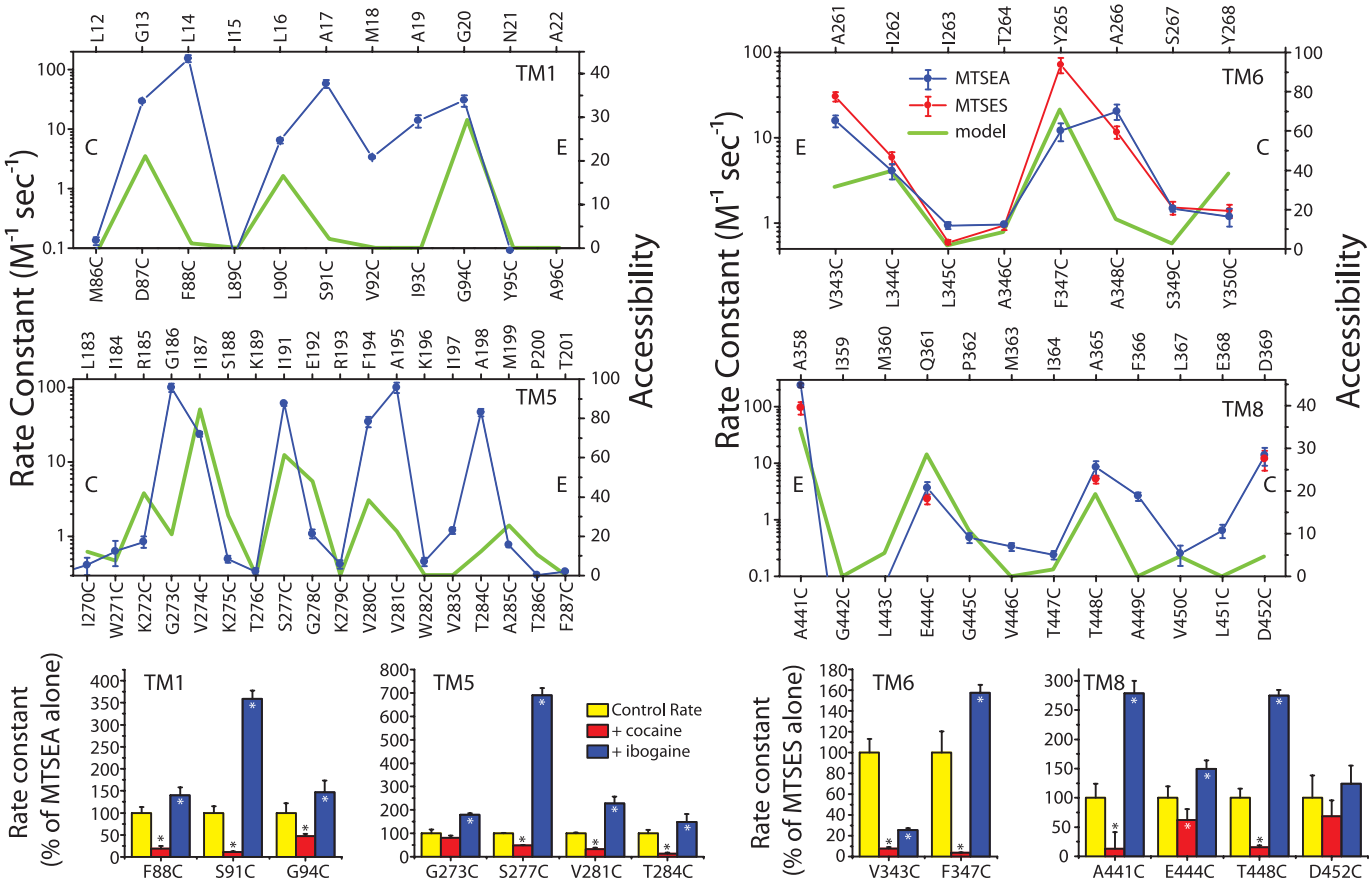

Fig. 2. Rate constants for reactivity of cytoplasmic pathway mutants with MTS reagents. (*Upper*) Calculated rate constants for inactivation of β-CIT binding to the indicated mutants by MTSEA (and MTSES for TMs 6 and 8). Bottom axes are SERT positions, and corresponding residues in LeuT are shown on the top axes (15). C and E indicate the cytoplasmic and extracellular ends, respectively, of each region. The green line indicates the accessibility in the cytoplasm-facing state model. The solvent-accessible surface area (SASA) for each residue was calculated as a percentage of the SASA of the same amino acid type (X) in a reference gly-X-gly tripeptide. From this, the equivalent percentage in the crystal structure was subtracted, so that the accessibility is positive only for residues that are exposed in the cytoplasm-facing state model; for all other residues, the accessibility is zero. Mutants with the highest rates of inactivation were further tested by measuring inactivation rates in the presence of 10 μM cocaine or ibogaine. (*Lower*) Rates of inactivation, relative to rates with the MTS reagent alone, for these selected positions. Error bars indicate the standard error of the means from three independent experiments. Asterisks indicate a significant difference from the control rate with MTS reagent alone ($P < 0.05$, paired Student's t test). TM5 data are from (20, 21).

connected to the rest of the protein by three extramembranous loops (Fig. 1, yellow and orange). Note that the bundle contains two helices from each of the two structural repeats. The remainder of the protein, composed of the last three helices of each structural repeat, TMs 3–5 and 8–10 (and TMs 11–12), forms a sort of scaffold around the TM 1-2-6-7 bundle (Fig. 1, light blue and dark blue). The asymmetry observed in Fig. 4 results in an orientation of the bundle relative to the scaffold in which the cytoplasmic end packs against TM5 and -8, sealing off the binding site from the cytoplasm, whereas the extracellular end of the bundle tilts away from TMs 3 and 10, allowing extracellular access almost to the binding site (Figs. 1*B* and 5*A*). Thus, it is precisely the difference in the conformations of the two structural repeats that is responsible for the formation of an asymmetric, extracellular-facing conformation (Fig. 5*A*). We reasoned that if the orientation of the bundle dictated access to the binding site, then the cytoplasm-facing state of LeuT, which releases substrate to the cytoplasm, would be formed by movement of the bundle during transport so as to block extracellular access and open cytoplasmic access to the binding site. We reasoned further that this repositioning would entail coordinated, complementary changes in both structural repeats—in effect, exchanging their conformations.

To test this hypothesis, we generated a model for the cytoplasm-facing state, which assumes that the two repeats, involving TMs 1–5 and TMs 6–10, switch conformations (see *SI Text*). That is, the sequence of TMs 1–5 adopts the conformation of TMs 6–10 and vice versa while keeping their original transmembrane topology. Minor adjustments of the alignment between the repeats (See *Methods* and *SI Text*) were required to retain the relationship of the residues involved in sodium and leucine binding and to maximize interaction of highly conserved residues with the rest of the protein rather than with solvent. In the resulting model (Fig. 5*B*), the extracellular end of the bundle is closer to TM3 and -10, and the cytoplasmic end of the bundle is further from TMs 5 and 8, breaking the Arg-5/Asp-369 ion pair at the cytoplasmic surface and effectively opening an aqueous pathway from the cytoplasm to the substrate binding site. The primary difference between this model and the crystal structure is that the TM1-2-6-7 bundle has rotated ≈25° around an axis in the membrane plane that runs through the Cα atom of Ser-256.

The LeuT Model Is Compatible with SERT Accessibility Data. The model predicts that in the cytoplasm-facing state, residues in TM1, -5, -6, and -8 become solvent-accessible with a helical periodicity, as found in accessibility studies (Fig. 2). Using that accessibility data, we refined the alignment of TM1a, -5, and -6b

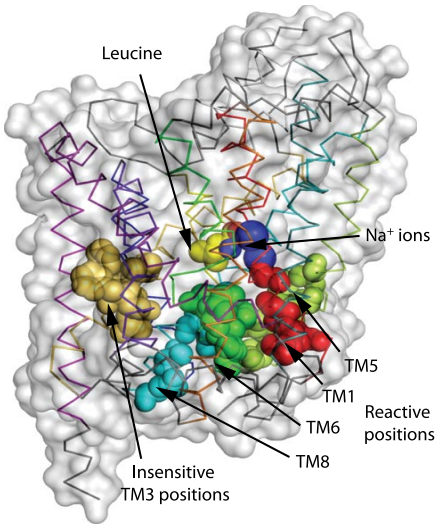

Fig. 3. Identification of the cytoplasmic permeation pathway in SERT. Residues in TM1 (red), -5 (lime), -6 (green), and -8 (cyan) of LeuT that correspond to those demonstrated by accessibility measurements (Fig. 2) to line the cytoplasmic pathway of SERT are shown as space-filling spheres. Five positions in TM3 with low accessibility (tan) are also shown. The C-alpha chain of LeuT (pdb code 2a65) is indicated by using the color coding of Yamashita *et al.* (9) along with a transparent representation of the protein surface.

(Fig. S3) to maximize exposure of the positions corresponding to the reactive residues in SERT (see *SI Text*). The resulting cytoplasm-facing state model of LeuT retains the overall conformation shown in Fig. 5*B*, while the calculated accessibility peaks at or adjacent to corresponding positions in SERT that showed the greatest exposure to intracellular MTSEA (Fig. 2 *Upper*, green line). In support of this refined model, two of the positions predicted to face the permeation pathway correspond to endogenous cysteines in TMs 1 and 6 of the homologous tyrosine transporter Tyt1 that were shown to become accessible as a consequence of substrate transport (28).

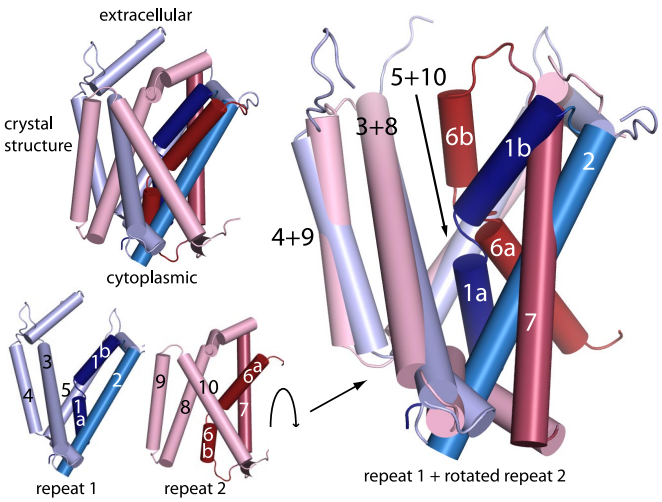

Fig. 4. Structural asymmetry of repeats in LeuT. TMs 1–10 of the LeuT crystal structure (*Upper Left*) were separated into the two structural repeats (*Lower Left*). TMs 1–2, dark blue; TMs 3–5, pale blue; TMs 6–7, dark red; TMs 8–10, pale red. The repeats were superimposed by aligning the positions of the last three helices in each repeat (*Right*). This required an ≈180° rotation of repeat 2 with respect to repeat 1 as calculated with SKA (45). Note the different orientation of the first two helices (particularly 1 and 6) in each repeat with respect to the other three helices.

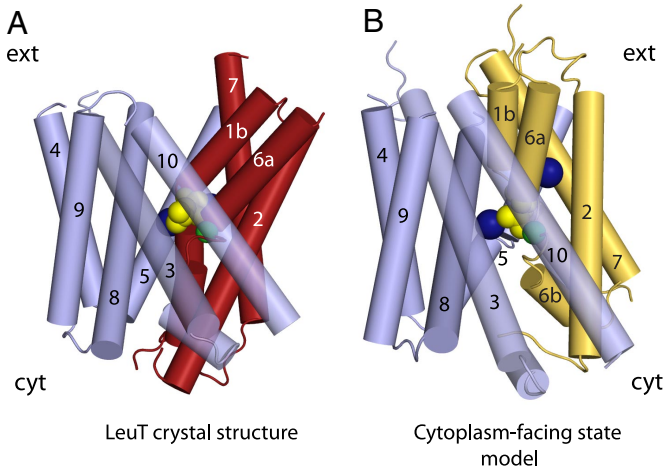

Fig. 5. Predicted conformational change in LeuT. The position of the four-helix bundle comprised of TMs 1–2 and 6–7 with respect to the scaffold (in blue) is shown along the plane of the membrane in red in the crystal structure (*A*) and in yellow in the model of the cytoplasm-facing state (*B*). The positions of the sodium ions (blue), the leucine substrate (yellow), and the Cα-atom of Ser-256 (green) are shown as spheres. For clarity, TM11 and -12 and the extracellular loops are not shown.

Fig. 6 shows a cytoplasmic surface view of the LeuT crystal structure and the cytoplasm-facing state model with residues corresponding to the highly reactive positions of SERT labeled in red or orange. In addition, the leucine and sodium ions bound at the active site are labeled in yellow and blue, respectively. This model exposes to the solvent most of the residues corresponding to the reactive SERT positions (16 of 21 are accommodated by the model and three more are at adjacent positions) and exposes leucine and the sodium ion designated as Na2 by Yamashita *et al.* (9). Although not visible, Na1 is separated from the solvent only by the bound leucine molecule. The positions in TM3 of SERT where a cysteine did not increase sensitivity to MTSEA (Fig. 3) notably remained buried in this model. Finally, the model of the cytoplasm-facing state also predicts closure of the extracellular pathway, which is shown in Fig. 5*B* and Fig. S4 and was demonstrated experimentally in refs. 21, 26, 29, and 30.

Discussion

The results presented here identify the residues that form a permeation pathway in SERT through which bound substrate may dissociate to the cytoplasm. They also provide a model for the cytoplasm-facing state of LeuT in which this cytoplasmic permeation pathway is open. We took advantage of the high-resolution structure of LeuT as a basis for modeling and exploited the ability of cocaine and ibogaine to manipulate the conformation of SERT as support for the model. The high degree of correspondence between the residues that constitute the cytoplasmic pathway of the model and the reactive residues in SERT (Figs. 2 and 6) provides a measure of confidence that the model approximates a permeation pathway common to LeuT, SERT and probably the entire family of NSS transporters. The difference between the crystal structure and the model represents a conformational change that may correspond to a general alternating-access mechanism in the NSS family. This conformational change, which exploits the internal symmetry of the LeuT structure, involves a net rotation of the four-helix bundle composed of TM1, -2, -6, and -7 around an axis close to the substrate and ion binding sites.

Rotation of the TM1-2-6-7 bundle in the model (Fig. 5) suggests a mechanism of substrate transport in which rocking of the bundle alternately opens and closes the cytoplasmic and

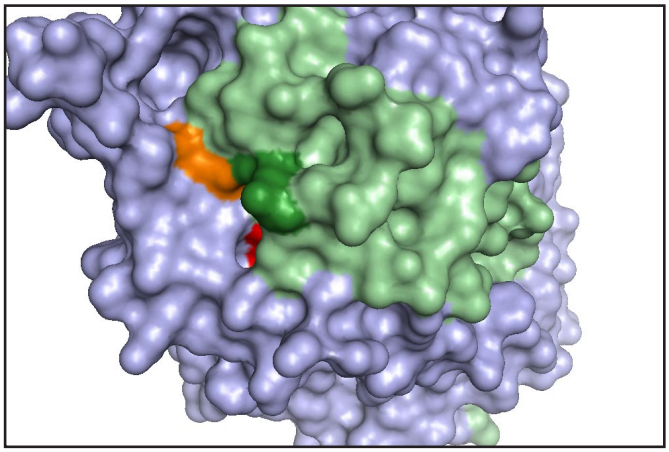

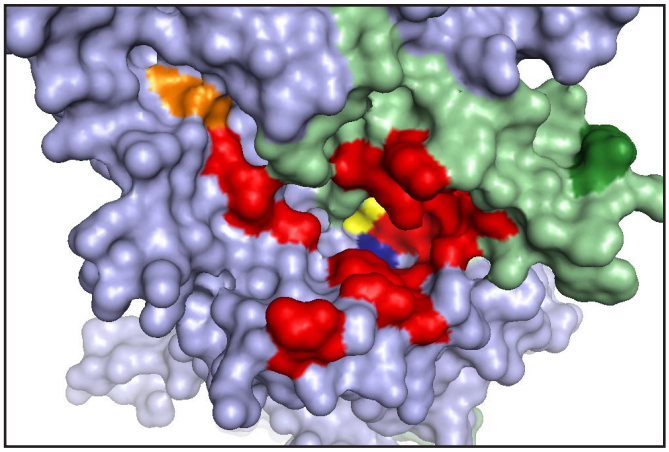

Fig. 6. Molecular surface of LeuT, viewed from the cytoplasmic side of the membrane. (*Upper*) X-ray crystal structure. (*Lower*) Model of the cytoplasm-facing state. The bundle is shaded light green and the remainder of the protein light blue. The surface of leucine (yellow), Na2 (blue), the Arg-5 (green), and Asp-369 (orange) ion pair and residues corresponding to those found to be accessible in SERT (red and orange) are highlighted.

extracellular permeation pathways. This rearrangement occurs on the side of the protein opposite from TM9 and -12 (which form a dimer interface in the LeuT crystal) and, therefore, would not be expected to interfere with oligomerization (see Fig. 1). According to the alternating access model, the changes in accessibility should occur without disrupting substrate and ion binding. Therefore, it is significant that the bundle residues that change position the least between the crystal structure and the model are located close to the substrate and ion binding sites (Fig. S5). We speculate that the strong polar and ionic interactions between TM1, -6, and -8 that are mediated through bound solutes may help to define the axis about which the bundle rotates. In particular, Na2 interacts with three backbone carbonyl oxygens from TMs 1 and 8 and two hydroxyl oxygens from TM8 (i.e., from within the TM1-2-6-7 bundle and from TM8 in the scaffold). The presence of two sodium sites, which are conserved even in SERT, where only one sodium is cotransported (31, 32), raises the possibility that Na2 is not released but instead functions as a nexus for strong ionic interactions that define a hinge region between the bundle and the remainder of the protein.

Although no specific models for the cytoplasm-facing state have been proposed, Gouaux and coworkers (9, 16) did suggest, in agreement with our model, that TM1 and -6 might rearrange during the transport cycle, moving together to change binding site accessibility. We do not rule out their suggestion that this rearrangement involves a series of transient steps in which unwound regions of TM1 and -6 act as joints or that TM3, -5, -8, -10, and -11 move significantly (9, 16). However, our data may be explained more simply by the movement of TM1, -2, -6, and -7 as a unit with little additional conformational change. The proposal that the bundle moves as a unit is consistent with the observation that the loops between TMs 1-2 and 6-7 (i.e., within the bundle) are short and highly conserved, allowing the helices to maintain their relative positions, whereas the loops between the bundle and the scaffold are long, and contain short extramembranous helices.

Although our model may not be accurate with respect to the details of binding site interactions and minor movements of other helices, it provides the first structural description of the overall architecture of the cytoplasm-facing state for the NSS transporter family. The inherent pseudo twofold symmetry in the structure is not reflected at the sequence level in this family, so that different residues are involved in extracellular and cytoplasmic permeation pathways. Nevertheless, the model derived from the structural symmetry is consistent with accessibility measurements at 54 different positions in TM1, -3, -5, -6, and -8, indicating that it provides a strong basis for future experimental and computational studies on the structural basis of the transport mechanism.

Both the accessibility studies and the modeling in this work resulted from an appreciation of the role that symmetry, inherent in the structure of LeuT, might play in the mechanism of transport. At present, little is known of the conformational mechanisms for transport proteins. Although it is not yet clear how general the mechanism proposed here will prove to be, we anticipate that analysis of conformational differences between topologically inverted structural repeats may give insight into transport mechanisms in other families. Inverted repeats have been observed in crystal structures from other membrane transport proteins (5, 10, 11, 33). Moreover, structure and sequence analysis (22) suggests that additional transport families are constructed from repeating elements, each containing an odd number of transmembrane helices, implying that the repeats have opposite topologies (34–39). In the case of SMR proteins, the inverted repeat structure may be formed by two polypeptide chains with opposite topology (40, 41). We anticipate that analysis of structures from those families, coupled with accessibility measurements, may reveal their conformational mechanisms also. Preliminary computational results with the ClC_{ec} structure (10) point to a conformational asymmetry between repeats in a region that interacts with bound Cl^- (L.R.F., unpublished observations). The inverted structural repeat may thus represent a general solution to alternating access that is used by many proteins that catalyze topologically symmetrical vectorial transport reactions.

Methods

MTS Reactivity Measurements. Mutations were generated in rat SERT and sequenced as described in ref. 19. Each mutant was tested for transport activity and sensitivity to MTS reagents by transfecting HeLa cells with plasmids bearing each mutant cDNA under control of a T7 promoter and infecting with vTF7–3, a recombinant vaccinia virus expressing bacteriophage T7 RNA polymerase (42). Transport activities and sensitivity to 1 mM MTSEA in these intact cells are shown in Table S1. Membranes were prepared from transfected cells, and β-CIT binding was measured as described in ref. 43. Binding to membranes was measured before and after incubation with MTSEA or MTSES (19), and typical results are shown in Fig. S1. When present, cocaine or ibogaine were added just before addition of MTS reagent. Rate constants for inactivation were calculated from the concentrations of MTS reagent yielding half-maximal inactivation of β-CIT binding activity in a 15-min incubation (20).

Modeling. A model of the cytoplasm-facing conformation of LeuT was constructed by using Modeller software, Version 6.2 (44), using the crystal structure as a template. The alignment (Fig. S3) was obtained from structural superposition, using SKA (45) of the two repeat units of the LeuT structure. Thus, residues in the first repeat were modeled by using the structure of the second repeat as a template and vice versa. More details are provided in *SI Text*.

Note Added in Proof. Shi *et al.* (46) recently proposed a cytoplasmic permeation pathway in LeuT, based on steered molecular dynamic simulations. The pathway they propose involves only small changes in protein conformation relative to the crystal structure, whereas our proposed pathway requires significant movement of the 1-2-6-7 bundle. The pathway of Shi *et al.* is formed from some of the same positions in TMs 1, 5, 6, and 8 that were identified as accessible in our study (corresponding to A17, I187, I191, A195, A261, I262, Y265, A358, and Q361 in LeuT). However, their proposed path does not include many other residues corresponding to accessible SERT positions (G13, L14, G20, G186, F194, A198, A266, A365, and D369) and includes L183, which corresponds to a position in SERT only weakly reactive toward MTSEA (Fig. 2).

Faham *et al.* (47) showed that the structure of vSGLT, a transporter in the SSS family, resembles that of LeuT. In that structure, the scaffold region in vSGLT appears to be essentially conserved compared with LeuT, whereas TMs 2, -3, -7, and -8, which correspond to the TM1-2-6-7 bundle of LeuT, also form a unit together with TM14, a helix that does not correspond to any helix of LeuT. Furthermore, vSGLT is in a cytoplasm-facing conformation, revealing a pathway highly consistent with that identified here in SERT. Superimposing the inverted repeats of vSGLT (TMs 2-6 and TMs 7-11) as in Fig. 4 reveals a difference in the conformation of the first two helices in each repeat as in LeuT. Although the arrangement of the helices on the extracellular side of the vSGLT structure differ from our model, it appears that the general mechanism we propose here for the NSS family may also be relevant for the SSS and possibly additional transporter families.

ACKNOWLEDGMENTS. We thank Jeff Abramson and Ernest Wright for a preprint of ref. 47 and coordinates of the vSGLT structure. L.F. thanks J. Faraldo-Gómez, D. Petrey, and C. Tang for helpful discussions. This work was supported by National Institute on Drug Abuse Grants DA007259, DA008213, and DA012408 (to G.R.); National Science Foundation Grant MCB-0416708 (to B.H.); and National Institutes of Health Grant U54 GM75026 (to B.H.).

1. Jardetzky, O (1966) Simple allosteric model for membrane pumps. *Nature* 211:969–970.
2. Takahashi M, Kondou Y, Toyoshima C (2007) Interdomain communication in calcium pump as revealed in the crystal structures with transmembrane inhibitors. *Proc Natl Acad Sci USA* 104:5800–5805.
3. Olesen C, *et al.* (2007) The structural basis of calcium transport by the calcium pump *Nature* 450:1036–1042.
4. Hirai T, *et al.* (2002) Three-dimensional structure of a bacterial oxalate transporter. *Nat Struct Biol* 9:597–600, 2002.
5. Abramson J, *et al.* (2003) Structure and mechanism of the lactose permease of Escherichia coli. *Science* 301:610–615.
6. Pebay-Peyroula E, *et al.* (2003) Structure of mitochondrial ADP/ATP carrier in complex with carboxyatractyloside *Nature* 426:39–44.
7. Huang Y, Lemieux MJ, Song J, Auer M, Wang D-N (2003) Structure and mechanism of the glycerol-3-phosphate transporter from Escherichia coli. *Science* 301:616–620.
8. Yernool D, Boudker O, Jin Y, Gouaux E (2004) Structure of a glutamate transporter homologue from Pyrococcus horikoshii. *Nature* 431:811–818.
9. Yamashita A, Singh SK, Kawate T, Jin Y, Gouaux E (2005) Crystal structure of a bacterial homologue of Na^+/Cl^--dependent neurotransmitter transporters. *Nature* 437:215–223.
10. Dutzler R, Campbell EB, Cadene M, Chait BT, MacKinnon R (2002) X-ray structure of a ClC chloride channel at 3.0 Å reveals the molecular basis of anion selectivity. *Nature* 415:287–294.
11. Hunte C, *et al.* (2005) Structure of a Na^+/H^+ antiporter and insights into mechanism of action and regulation by pH. *Nature* 435:1197–1202.
12. Kaback HR, *et al.* (2007) Site-directed alkylation and the alternating access model for LacY. *Proc Natl Acad Sci USA* 104:491–494.
13. Majumdar DS, *et al.* (2007) Single-molecule FRET reveals sugar-induced conformational dynamics in LacY. *Proc Natl Acad Sci* 104:12640–12645.
14. Smirnova I, *et al.* (2007) Sugar binding induces an outward facing conformation of LacY. *Proc Natl Acad Sci* 104:16504–16509.
15. Beuming T, Shi L, Javitch JA, Weinstein H (2006) A comprehensive structure-based alignment of prokaryotic and eukaryotic neurotransmitter/Na^+ symporters (NSS) aids in the use of the LeuT structure to probe NSS structure and function. *Mol Pharmacol* 70:1630–1642.
16. Singh S, Yamashita A, Gouaux E (2007) Antidepressant binding site in a bacterial homologue of neurotransmitter transporters. *Nature* 448:952–956.
17. Zhou Z, *et al.* (2007) LeuT-desipramine structure reveals how antidepressants block neurotransmitter reuptake. *Science* 317:1390–1393.
18. Keller PC, II, Stephan M, Glomska H, Rudnick G (2004) Cysteine-scanning mutagenesis of the fifth external loop of serotonin transporter. *Biochemistry* 43:8510–8516.
19. Zhang YW, Rudnick G (2005) Cysteine scanning mutagenesis of serotonin transporter intracellular loop 2 suggests an alpha-helical conformation. *J Biol Chem* 280:30807–30813.
20. Zhang YW, Rudnick G (2006) The cytoplasmic substrate permeation pathway of serotonin transporter. *J Biol Chem* 281:36213–36220.
21. Jacobs MT, Zhang Y-W, Campbell SD, Rudnick G (2007) Ibogaine, a noncompetitive inhibitor of serotonin transport, acts by stabilizing the cytoplasm-facing state of the transporter. *J Biol Chem* 282:29441–29447.
22. Saier MH (2003) Tracing pathways of transport protein evolution. *Mol Microbiol* 48:1145–1156.
23. Shimizu T, Mitsuke H, Noto K, Arai M (2004) Internal gene duplication in the evolution of prokaryotic transmembrane proteins. *J Mol Biol* 339:1–15.
24. Androutsellis-Theotokis A, Rudnick G (2002) Accessibility and conformational coupling in serotonin transporter predicted internal domains. *J Neurosci* 22:8370–8378.
25. Holmgren M, Liu Y, Xu Y, Yellen G (1996) On the use of thiol-modifying agents to determine channel topology. *Neuropharmacology* 35:797–804.
26. Henry LK, Adkins EM, Han Q, Blakely RD (2003) Serotonin and cocaine-sensitive inactivation of human serotonin transporters by methanethiosulfonates targeted to transmembrane domain I. *J Biol Chem* 278:37052–37063.
27. Stauffer DA, Karlin A (1994) Electrostatic potential of the acetylcholine binding sites in the nicotinic receptor probed by reactions of binding-site cysteines with charged methanethiosulfonates. *Biochemistry* 33:6840–6849.
28. Quick M, *et al.* (2006) State-dependent conformations of the translocation pathway in the tyrosine transporter Tyt1, a novel neurotransmitter : Sodium symporter from Fusobacterium nucleatum. *J Biol Chem* 281:26444–26454.
29. Mitchell SM, Lee E, Garcia ML, Stephan MM (2004) Structure and function of extracellular loop 4 of the serotonin transporter as revealed by cysteine-scanning mutagenesis. *J Biol Chem* 279:24089–24099.
30. Chen JG, Rudnick G (2000) Permeation and gating residues in serotonin transporter. *Proc Natl Acad Sci USA* 97:1044–1049.
31. Talvenheimo J, Fishkes H, Nelson PJ, Rudnick G (1983) The serotonin transporter-imipramine ''receptor'': Different sodium requirements for imipramine binding and serotonin translocation. *J Biol Chem* 258:6115–6119.
32. Quick MW (2003) Regulating the conducting states of a mammalian serotonin transporter. *Neuron* 40:537–549.
33. Fu D, *et al.* (2000) Structure of a glycerol-conducting channel and the basis for its selectivity. *Science* 290:481–486.
34. Saaf A, Baars L, von Heijne G (2001) The internal repeats in the $Na^+/Ca2^+$ exchanger-related Escherichia coli protein YrbG have opposite membrane topologies. *J Biol Chem* 276:18905–18907.
35. Jack DL, Yang NM, Saier MH, Jr (2001) The drug/metabolite transporter superfamily. *Eur J Biochem* 268:3620–3639.
36. Kimball RA, Martin L, Saier MH, Jr (2003) Reversing transmembrane electron flow: the DsbD and DsbB protein families. *J Mol Microbiol Biotechnol* 5:133–149.
37. Minocha R, Studley K, Saier MH, Jr (2003) The urea transporter (UT) family: Bioinformatic analyses leading to structural, functional, and evolutionary predictions. *Receptors Channels* 9:345–352.
38. Khademi S, *et al.* (2004) Mechanism of ammonia transport by Amt/MEP/Rh: Structure of AmtB at 1.35 Å. *Science* 305:1587–1594.
39. Dumay QC, Debut AJ, Mansour NM, Saier MH, Jr (2006) The copper transporter (Ctr) family of Cu^+ uptake systems. *J Mol Microbiol Biotechnol* 11:10–19.
40. Rapp M, Seppala S, Granseth E, von Heijne G (2007) Emulating membrane protein evolution by rational design. *Science* 315:1282–1284.
41. Schuldiner S (2007) When biochemistry meets structural biology: The cautionary tale of EmrE. *Trends Biochem Sci* 32:252–258.
42. Blakely RD, Clark JA, Rudnick G, Amara SG (1991) Vaccinia-T7 RNA polymerase expression system: Evaluation for the expression cloning of plasma membrane transporters. *Anal Biochem* 194:302–308.
43. Chen JG, Sachpatzidis A, Rudnick G (1997) The third transmembrane domain of the serotonin transporter contains residues associated with substrate and cocaine binding. *J Biol Chem* 272:28321–28327.
44. Fiser A, Sali A (2003) Modeller: Generation and refinement of homology-based protein structure models. *Methods Enzymol* 374:461–491.
45. Petrey D, Honig B (2003) GRASP2: Visualization, surface properties, and electrostatics of macromolecular structures and sequences. *Methods Enzymol* 374:492–509.
46. Shi L, Quick M, Zhao Y, Weinstein H, Javitch JA (2008) The mechanism of a neurotransmitter:sodium symporter—Inward release of Na^+ and substrate is triggered by substrate in a second binding site. *Molecular Cell* 30:667-677.
47. Faham S, *et al.* (2008) The crystal structure of a sodium galactose transporter reveals mechanistic insights into Na^+/sugar symport. *Science*, 10.1126/science.1160406.